Infrared Physics & Technology 76 (2016) 691–697

Contents lists available at ScienceDirect

Infrared Physics & Technology

journal homepage: www.elsevier.com/locate/infrared

Regular article

Guided filter and adaptive learning rate based non-uniformity correction algorithm for infrared focal plane array

Rong Sheng-Hui [a], Zhou Hui-Xin [a,*], Qin Han-Lin [a], Lai Rui [b], Qian Kun [a]

[a] School of Physics and Optoelectronic Engineering, Xidian University, Xi'an, Shaanxi 710071, China
[b] School of Microelectronics, Xidian University, Xi'an, Shaanxi 710071, China

ARTICLE INFO

Article history:
Received 26 August 2015
Accepted 28 April 2016
Available online 3 May 2016

Keywords:
Infrared focal plane array
Non-uniformity correction
Neural network
Guided filter
Adaptive learning rate

ABSTRACT

Imaging non-uniformity of infrared focal plane array (IRFPA) behaves as fixed-pattern noise superimposed on the image, which affects the imaging quality of infrared system seriously. In scene-based non-uniformity correction methods, the drawbacks of ghosting artifacts and image blurring affect the sensitivity of the IRFPA imaging system seriously and decrease the image quality visibly. This paper proposes an improved neural network non-uniformity correction method with adaptive learning rate. On the one hand, using guided filter, the proposed algorithm decreases the effect of ghosting artifacts. On the other hand, due to the inappropriate learning rate is the main reason of image blurring, the proposed algorithm utilizes an adaptive learning rate with a temporal domain factor to eliminate the effect of image blurring. In short, the proposed algorithm combines the merits of the guided filter and the adaptive learning rate. Several real and simulated infrared image sequences are utilized to verify the performance of the proposed algorithm. The experiment results indicate that the proposed algorithm can not only reduce the non-uniformity with less ghosting artifacts but also overcome the problems of image blurring in static areas.

1. Introduction

Infrared focal plane arrays (IRFRA) imaging system has tremendous value on both military and civilian applications. However, at present due to the immature manufacturing process, the response under the same infrared irradiance varies between the different detection element within an IRFPA. This phenomenon will impose the fixed pattern noise (FPN) in the infrared image which is called non-uniformity of IRFRA [1], and the non-uniformity has a serious impact on the sensitivity and the quality of IRFPA imaging system. Thus it is very essential to develop an effective non-uniformity correction (NUC) algorithm to achieve higher quality infrared images.

The NUC algorithm aims to eliminate the unwanted FPN and recovery the real infrared image. It is generally identified into two main categories, the reference-based non-uniformity correction (RBNUC) and the scene-based non-uniformity correction (SBNUC). RBNUC methods mainly contains two-point correction and multi-point correction methods [2], and etc. These methods employ uniform blackbody as reference irradiance sources to calculate the correction parameter. The advantages of these methods lie in its simplicity and low computational complexity. However, its correction process must be repeated because of the temporal drift of the response characteristic parameter of IRFPA. This procedure may also reduce the reliability of the infrared system and increase its maintenance costs.

On the other hand, the correction parameter of SBNUC usually depends on the information of the imaging scene, which has highly application value. Moreover, the non-uniformity is corrected during the normal operation of the imaging system, which would reduce the operation complexity and avoid imaging interruption. Some SBNUC methods have been proposed over the years, and these methods can be broadly classified into four categories which are the statistics based method, the temporal filtering based method, the registration based method and the optimal estimation based method. Several typical methods of SBNUC are introduced as follow.

(1). The Constant statistics (CS) based method [3] assumes that the temporal mean and variance of each pixel are identical, however it heavily relies on the scene moving and have to spend much time to converge.

* Corresponding author.
E-mail address: hxzhou@mail.xidian.edu.cn (Z. Hui-Xin).

http://dx.doi.org/10.1016/j.infrared.2016.04.037
1350-4495/

(2). The temporal high-pass filtering (THP) based method [4] sets a high-pass filtering in the temporal domain and the FPN will be removed due to its low-frequency characteristic. However, The THP method will remove the static object and cause serious ghosting artifact. Although the spatial low-pass and the temporal high-pass NUC methods [5] apply a solution to solve this problem, the gain of FPN still cannot been removed. Besides, the cut-off frequency of the spatial filter and the temporal filter are difficult to determine as well.

(3). The registration-based method [6,7] considers that different infrared detection elements should have identical response when observing the same scene position and the difference response between them is mainly caused by the FPN. However the accuracy of registration affects the NUC performance seriously. Thus it is hard to employ this approach to correct the imaging scene with a weak infrared radiation or less image detail feature.

(4). The optimal estimation based method mainly contains Neural network based (NN–NUC) [8], Kalman filter based [9,10] and particle filter based [11], and etc. the NN–NUC based methods are widely used because of its better adaptively and noise immunity. However, the traditional NN–NUC would result in ghosting artifact to the moving object and image blurring to static scene, which restrict its application.

Considering the drawbacks of the traditional NN–NUC methods, this paper proposes a novel NUC method based on the combination of an edge-preserve filter and the adaptive learning rate with temporal factor. Several real and simulated infrared sequences are adopted to test its performance, and experimental results indicate that this method can correct the non-uniformity effectively with few FPN residues left. Furthermore, the correction result of this method could be much closer to the real image.

The remainder is organized as follow. In Section 2, the mathematical model of non-uniformity and Scribner's NN–NUC algorithm are discussed. In Section 3, an improved method based on the guided filter to get desired image is proposed. In Section 4, an adaptive learning rate is introduced to protect static scene. In Section 5, the proposed algorithm is applied to several real and simulated infrared image sequences, and the conclusion is given in Section 6.

2. Related work

2.1. IRFPA and fixed pattern noise models

The response of each detection-element in an IRFPA can be approximated as a linear model, which is widely used and accepted. The linear model is defined as

$$x_{i,j}^n = a_{i,j}^n \cdot y_{i,j}^n + b_{i,j}^n \tag{1}$$

where n is the frame number, $x_{i,j}^n$ is the response of the detection-element (i, j), $y_{i,j}^n$ is the real infrared radiation received by the detection-element (i, j), $a_{i,j}^n$ and $b_{i,j}^n$ are the linear model parameters respectively. NUC algorithms aim to acquire the real value $y_{i,j}^n$ by estimating the correction coefficients from the raw value $x_{i,j}^n$.

$$\hat{y}_{i,j}^n = G_{i,j}^n \cdot x_{i,j}^n + O_{i,j}^n \tag{2}$$

where $\hat{y}_{i,j}^n$ is the estimated real radiation value, $G_{i,j}^n = 1/a_{i,j}^n$ and $O_{i,j}^n = -b_{(i,j)}^n/a_{(i,j)}^n$ are the NUC gain and offset correction coefficients respectively.

2.2. Neural network based NUC

In the NN–NUC method, every infrared pixel is treated as a neuron. Through a hidden layer, the pixel can be connected to its surround pixels. By this way, a desired output is estimated by the mean of the four nearest neighbor pixels and fed back to the upper layers of the network to calculate the correction coefficient. As the sense varies, the correction coefficient is updated by the steepest descent algorithm frame by frame in order to get the optimal correction result. The sketch map of the traditional NN–NUC method is indicated in Fig. 1.

In the traditional NN–NUC method, the desired output $f_{i,j}^n$ is estimated by the nearest 4 neighbor pixels.

$$f_{i,j}^n = \left(x_{i,j+1}^n + x_{i,j-1}^n + x_{i+1,j}^n + x_{i-1,j}^n\right)/4 \tag{3}$$

and the error function F is given by (the frame number and the pixel location are omitted)

$$F(G, O) = (G \cdot x + O - f)^2 \tag{4}$$

The steepest descent algorithm is applied to minimize the error function F and the iteration direction is given by the derivative of F (G, O)

$$\begin{cases} F_G = \frac{\partial F}{\partial G} = 2x \cdot (G \cdot x + O - f) = 2x \cdot (y - f) \\ F_O = \frac{\partial F}{\partial O} = 2(G \cdot x + O - f) = 2(y - f) \end{cases} \tag{5}$$

In the steepest descent algorithm, the parameters are updated recursively with a portion of each respective error gradient indicated as follows

$$\begin{cases} G_{n+1} = G_n - 2\alpha x(y - f) \\ O_{n+1} = O_n - 2\alpha(y - f) \end{cases} \tag{6}$$

where n is the frame number, α is a small positive parameter which controls the convergence step size.

3. The improved desired output

In summary, NN–NUC is a kind of iteration process which reduces the error function based on the feedback of the hidden layer frame by frame. An accurate desired image can keep the iteration process reducing the error in the right direction, while a rough would increase the correction errors. The traditional NN–NUC adopts the mean value of the four neighbor pixels as the desired output image. Although the mean filter is reasonable in certain smooth areas, it is not suitable for the infrared image with many details (i.e. edges). As the mean filter will cause gradient distortion and lose many detail features where the wrong correction coefficient would be generated. As the scene varies or the object moves in the image, the improper correction coefficient cannot be repaired immediately. As a result, the inappropriate correction coefficient will cause the ghosting artifact on the corrected image.

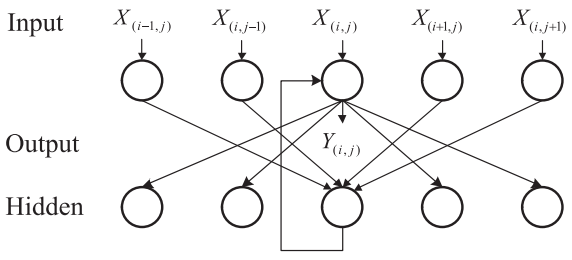

Fig. 1. Sketch map of the traditional NN–NUC method.

In order to illustrate the influence of the inaccurate desired image, a simulation experiments is implemented. In this experiment, a clear image sequence with a moving rectangle object is corrected by the NN–NUC method. A group of experimental result is shown in Fig. 2. Results indicate the effect of applying different mean filter window sizes in the NN–NUC method. As can been seen from Fig. 2, the mean filter would seriously decrease the correction effect, and the bigger the window size is, the worse the correction effect would achieve.

By analyzing the traditional NN–NUC, one effective way to decline the ghosting artifact is to acquire a more accurate desired imaged, especially for the image with strong edges. However both above mean filter and other linear filter will smooth the details in the image. The reason is that the filter weight is always the same in the whole image. Thus, a nonlinear filter, the guided filter, which could reserve the image details while reduce the FPN is adopted to solve this problem discussed above.

The guided image filter [12] is a kind of edge-preserve filter which can adjust the smooth degree based on the local characteristics of the image. Thus it can distinguish the edge and the smooth region in the image. By this filter, a desired image D_i with accurate details and less FPN can be gotten form the guidance image G_i by a local linear transformation

$$D_i = a_k G_i + b_k, \quad \forall i \in w_k \tag{7}$$

where w_k is a local rectangle window with size of $(2r+1)\times(2r+1)$. a_k and b_k are the transforming coefficient which could be solved by minimizing the following cost function

$$E(a_k,\ b_k) = \sum_{i\in w_k}\left((a_k G_i + b_k - P_i)^2 + \varepsilon \cdot a_k^2\right) \tag{8}$$

where ε is a regularization parameter penalizing large a_k and P_i is the original input image. Through the linear range regression algorithm, the linear coefficient a_k and b_k can be solved as

$$a_k = \frac{\frac{1}{|w|}\sum_{i\in w_k} G_i P_i - \mu_k \bar{P}_k}{\sigma_k^2 + \varepsilon} \tag{9}$$

$$b_k = \bar{P}_k - a_k \mu_k \tag{10}$$

where μ_k and δ_k are the mean and the variance of G in the local rectangle window w_k. $|w|$ is the number of pixel in w_k, and $\bar{P}_k$ is the mean of P in w_k. In this paper, the mean filter is replaced by the guided filter.

$$f = G_{r,\varepsilon}(P, G) \tag{11}$$

where operator $G_{r,\varepsilon}(P, G)$ represents the guided filter operation, r is the filter window and ε is the fuzzy degree factor, P is the input image and G is the guided image. In this paper, both P and G are the original infrared image with FPN. In this case, $a_k = \sigma_k^2/(\sigma_k^2+\varepsilon)$ and $b_k = (1-a_k)\mu_k$. If the image G changes a lot within w_k, there is $\sigma_k^2 \gg \sigma$, so $a_k \approx 1$ and $b_k \approx 0$. The filter can preserve most of details. If the image G is almost constant in w_k, there is $\sigma_k^2 \ll \sigma$, so $a_k \approx 0$ and $b_k \approx \mu_k$. The filter can remove the FPN as same as a mean filter.

In short, the guided filter can change the filter property based on the local characteristics of the input image. Thus, a more accurate desired image would be gotten which is helpful to decrease the effect of ghosting artifacts.

4. Improved adaptive learning rate

The learning rate is another important factor to achieve good correction results. As mentioned above, the learning rate α which controls the convergence speed in the Scribner's NN–NUC is fixed for the whole image. Generally, a larger α value can provide a faster convergence speed, while a smaller value can assure better stability instead. In the practical application, very small learning rate values are commonly used, leading to a very slow, but safe, convergence.

In order to achieve a higher performance, the local spatial standard deviation is used to measure the error confidence between the real infrared radiation and the desired image in the article [13]. In this way, each pixel has an independent adaptive learning rate $\alpha_{ij}(n)$ in the adaptive NUC neural network structure. So the learning rate could be adjusted specially based on the local information to improve the effect of the correction result.

However this method doesn't consider the movement of the object or the scene in the image. In the static areas with less detail, the learn rate would be larger than other places and the larger learning rate would lead serious image blurring because of the lack of scene information. While it is reasonable to select a larger learn rate to boost the correction rate for the moving object. Above all, a larger learning rate would accelerate the correction speed and decline the effect of ghosting artifact for the moving area or the object; a smaller learning has relative steady correction result. According to the analysis, combining the spatial characteristics with the movement information at the same time is an effective way to improve the result of non-uniformity correction. Thus, both the temporal and the local spatial standard deviation are selected to improve the adaptive learning rate in this paper.

$$\alpha_{ij}(n) = \frac{k\cdot\sigma_{ij}^T(n)}{1+\sigma_{ij}^S(n)} \tag{12}$$

where n is the frame number, k is a constant parameter, $\sigma_{ij}^S(n)$ is the local spatial standard deviation of the input image. $\sigma_{ij}^T(n)$ is the local temporal domain standard deviation defined as

$$\sigma_{ij}^T(n) = D\left[\{x_{ij}(n), x_{ij}(n-1), \ldots, x_{ij}(n-m+1)\}\right] \tag{13}$$

where m is the temporal parameter, the operator D indicates the operation of standard deviation.

In this method, the learning rate depends on not only the spatial information but also the movement information of the scene. As

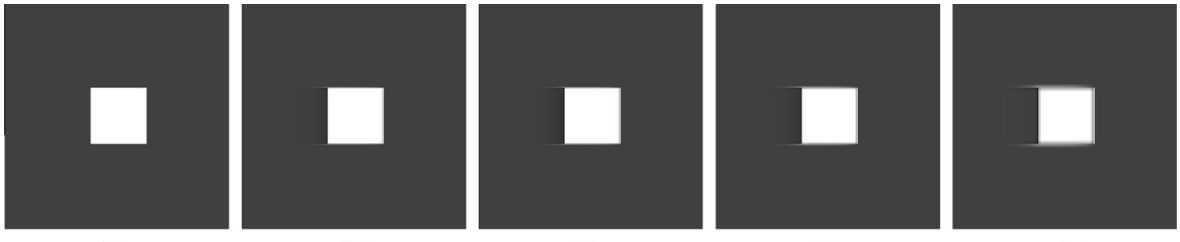

Fig. 2. The influence of inaccurate desired image. (a) Raw image, (b) four neighbor filter, (c) 3 × 3 mean filter, (d) 5 × 5 mean filter, and (e) 9 × 9 mean filter.

the scene varies, the temporal domain standard deviation would increase. So the moving object will get a larger learning rate, which could decline the effect of ghosting artifact. By contrast, when the scene changes slowly or remains static, the temporal domain standard deviation could maintain the learning rate in a small figure even zero, thus the correction parameter in this areas would remain unchanged or change slightly, which could decline the effect of image blurring and maintain image clear.

In summary, the flow chart of the proposed improved NUC is indicated in Fig. 3.

5. Experiment results and analysis

In order to indicate the effectiveness of the proposed algorithm for NUC, a real video sequence obtained by a long-wave uncooled infrared camera and three simulated sequences obtained in Vivid track data set are used to test the proposed algorithm. Our experiments evaluate the proposed algorithm and compare it with other four typical adaptive methods from literatures. These are:

(1). The classic adaptive retina-like non-uniformity correction (NN–NUC).
(2). The fast adaptive non-uniformity correction (FA–NUC). This method applies an adaptive step size which adjusts based on the local spatial standard deviation to control the learning rate. The fixed global parameter K_{alr} is set to 0.075.
(3). The bilateral filter based adaptive non-uniformity correction (BF–NUC) [14]. This method applies the bilateral filter to calculate the desired image. The mask dimension of bilateral filter, D, is set to 7 and the standard deviation of the spatial distances and the intensity dissimilarity are set to $D/6$ and 50/255 respectively.
(4). The total variation approach for adaptive non-uniformity correction (TV–NUC) [15], this method is a generalization of former adaptive NUC method based on neural networks. Comparatively performance of this approach confirms the adaptive characteristic in our proposed algorithm.

In the proposed algorithm, the guided filter window size r and fuzzy degree factor ε are set to 8 and 0.2 respectively, the time parameter m is set to 9, and the neighborhood of local spatial is set to 3×3, the gray range of image is set from 0 to 1.

5.1. The real infrared image experimental result and analysis

The first image sequence (200×200 pixels) is obtained by a uncool IRFPA system with a girl waving her hand iteratively in the sequence. There is a static desk in left bottom corner of the image. A group of experimental results are shown in Fig. 4.

It can be seen from the original image in Fig. 4(a), the stripe FPN influences the image quality seriously. The correction result of NN–NUC is indicated in Fig. 4(c). Compared with other mean filter, the mean of four neighbor pixels is a compromise approach. Though FPN in the image cannot be eliminated completely, this method can keep the image clear with less image blurring and ghosting artifact. The correction result of FA–NUC is indicated in Fig. 4(d). It is clear that all the static parts are either removed or distorted. What's worse, there is serious ghosting artifact in the moving area, such as the head and arm. The fast learning rate is utilized to get a well correction result in this method, and the learning rate depends on the local spatial standard deviation of the image. In this test image sequence, the contour of the girl has intense contrast with the background and the learning rate is small in this place, when the people move around, the error correction cannot be corrected immediately which is the cause of ghosting artifact.

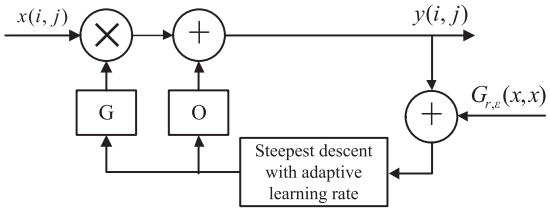

Fig. 3. Flow chart of the proposed improved desired image.

By contrast, the correction results of BF–NUC and TV–NUC are shown in Fig. 4(e) and (f) respectively. Thanks to the edge-preserve filter, the bilateral filter and the minimization of total variation algorithm, the ghosting is suppressed partially. However, the fixed learning rate restricts the convergence speed and make the static image blurring. The correction result of the proposed algorithm is indicated in Fig. 4(b). The stripe FPN is mostly removed and the ghosting artifact around the girl's head and arm cannot be seen any more. The result of the proposed algorithm has the best visual effect. Besides, all the static area of image is reserved completely. That is to say, the proposed algorithm can achieve well performance in subjective view.

5.2. The simulated experimental result and analysis

Due to the lack of public benchmark infrared sequence, in this section, three simulated sequences obtained in the public Vivid track data set (pktest01, pktest02 and pktest03, 320×256 pixels) with clear image and various scene are used for the NUC simulated experiment. In the typical IRFRA sensor, one column of pixels share the same amplifier and read-out circuit, so one column of pixels nearly have the same gain and offset FPN. Based on this assumption, a WGN (white Gaussian noise) stripe noise is use to simulate the infrared imaging non-uniformity, and the simulated FPN processing is indicated in Fig. 5. Both the gain and offset simulated parameter have the same value in column and follow a Gaussian distribution value in row, respectively.

In this section, two objective indicators are utilized to evaluate the quality of the correction results.

(1). *The roughness (ρ):* the smaller value of roughness represents the better correction result. This indicator partially reflect the visual effect of correction result and it is defined as

$$\rho = \frac{\|h_1 * x\|_1 + \|h_2 * x\|_1}{\|x\|_1} \tag{14}$$

where x is infrared image under analysis, $h_1 = [1, -1]$ is horizontal mask and $h_2 = h_1^T$ is vertical mask. $*$ indicates the discrete convolution operation; $\|\cdot\|_1$ indicates L1 norm.

(2). *The root-mean-square error (RMSE):* the difference between the corrected image and the real image. This indicator reflect the accuracy of correction result and it is defined as

$$RMSE = \sqrt{\frac{1}{m}\sum_{i=1}^{m}(y_i - x_i)^2} \tag{15}$$

where y is the corrected image and x is the real infrared image, and i is the i-th infrared pixel, m is the total number of pixel in the image.

A group of experimental results are shown in Figs. 6–8. Though the roughness is an objective indicator to illuminate the effectiveness of non-uniformity correction, it cannot reflect the de-ghosting and de-blurring effectiveness of the correction algorithm, which because the roughness in the blurring part of the image would be smaller than the other part. As can be seen from Figs. 6(a), 7(a) and 8(a), during the former 200 frames, the proposed algorithm

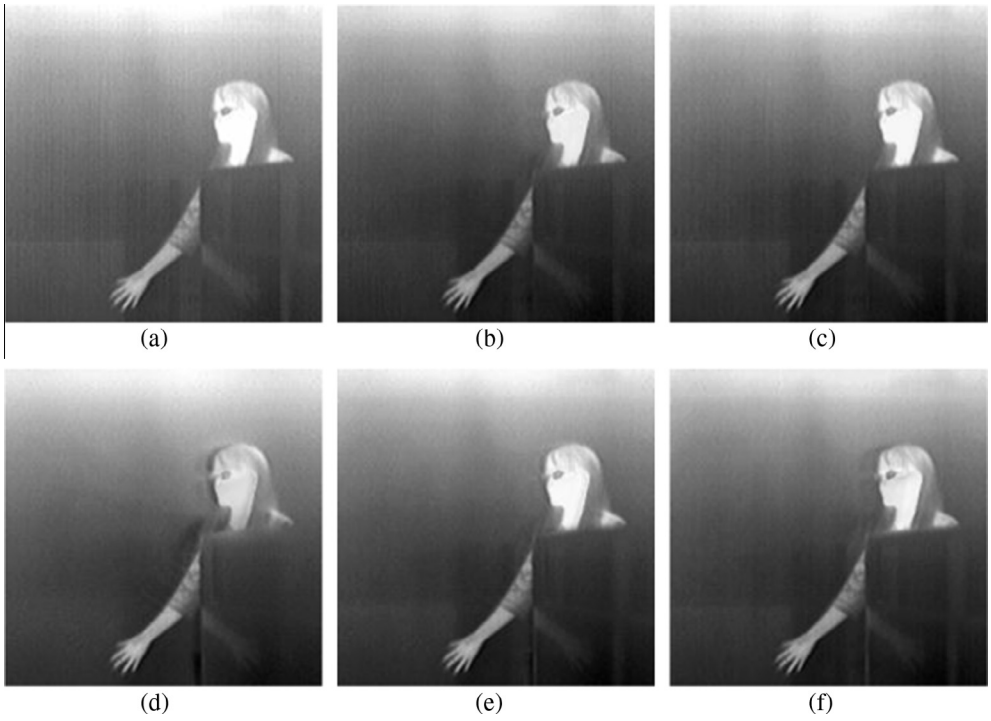

Fig. 4. Image filtering results. (a) Original image, (b) proposed algorithm, (c) NN–NUC, (d) FA–NUC, (e) BF–NUC, and (f) TV–NUC.

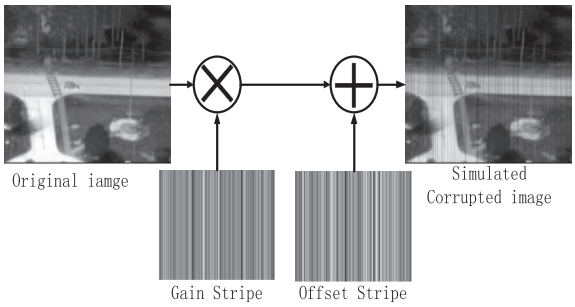

Fig. 5. The process of simulated FPN.

cannot get the smallest value of roughness compared with others. The reason is that the adaptive learning rate in the proposed algorithm is maintained in a small value in some static parts of the image where lack moving information, and other algorithms don't consider the movement of the object or the scene in the image which result in image blurring and a smaller roughness. After 400 frames, as the image scene varies, most areas of the image can get enough moving information. Thanks to the edge-preserve filter, the proposed algorithm has better capability to remove the FPN, as it has smaller figures of roughness.

From the RMSE figures, it can be seen that, compare to the other methods, RESE of the proposed algorithm is the smallest, which means its corrected result is the best. Moreover, the proposed algorithm has more steady convergence speed and can get more robust correction results.

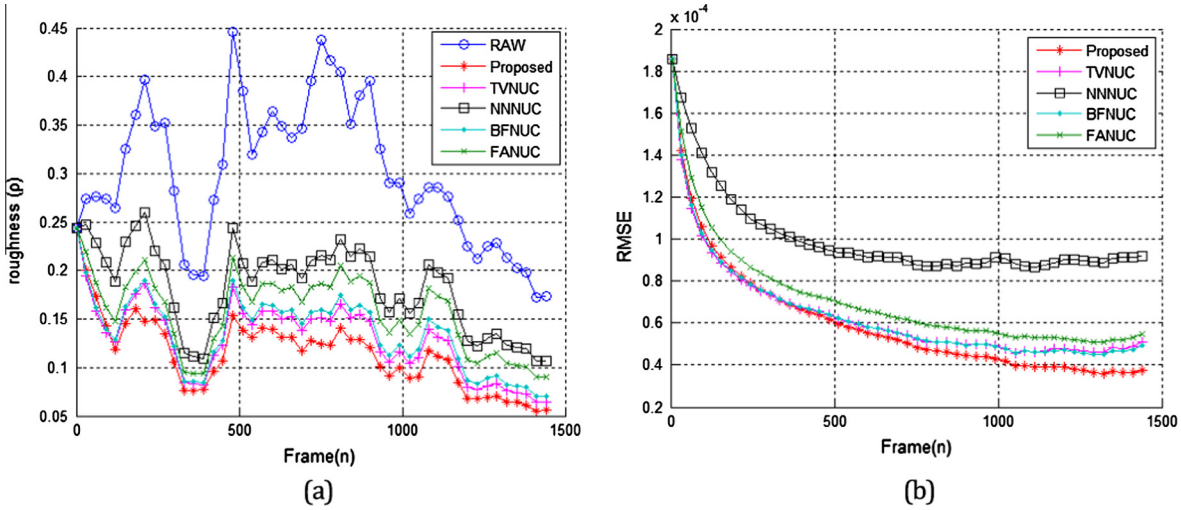

Fig. 6. Results of sequence pktest01. (a) Roughness and (b) RMSE.

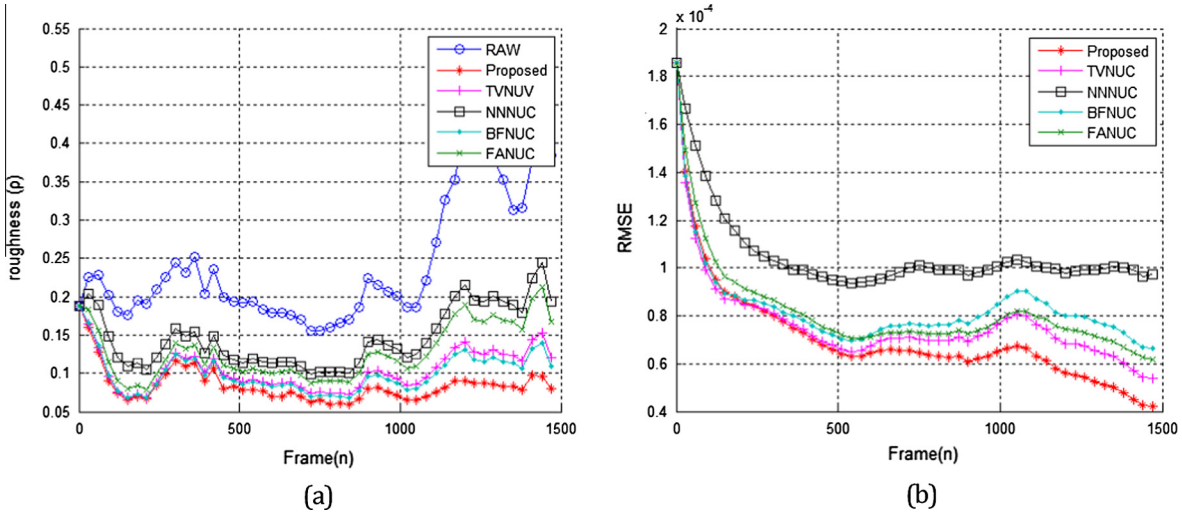

Fig. 7. Results of sequence pktest02. (a) Roughness and (b) RMSE.

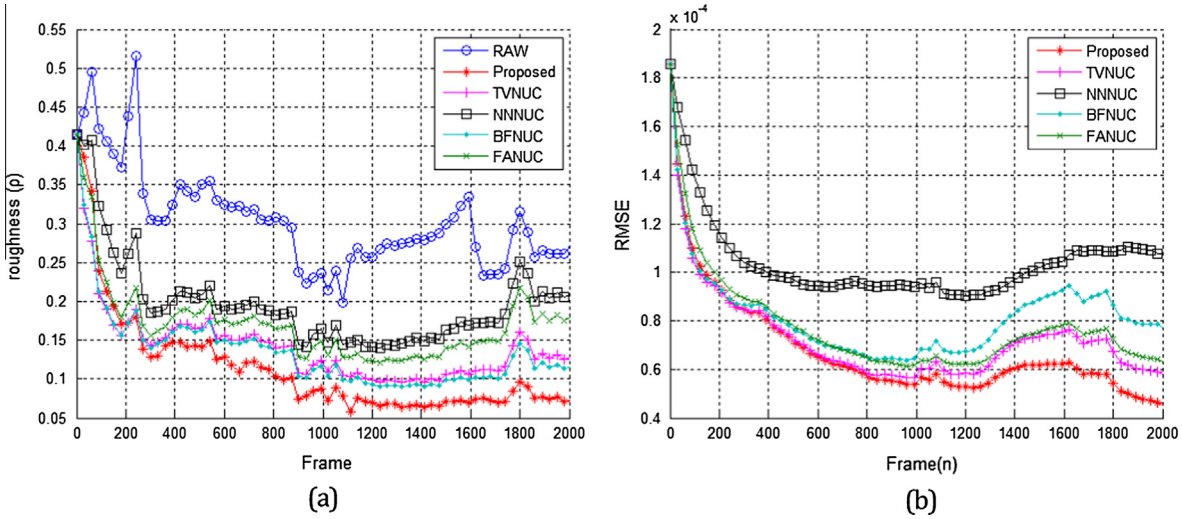

Fig. 8. Results of sequence pktest03. (a) Roughness and (b) RMSE.

In summary, these above-mentioned results indicate that the proposed algorithm balances the correction result and the visual effect, and has better performance of non-uniform correction in the aspects of both objective evaluation and subjective visual.

6. Conclusions

A useful method of the scene-based non-uniformity correction in IRFPA imaging system is proposed in this paper. By using an edge-preserve filter and an adaptive learning rate, the proposed algorithm can reduce the ghosting artifact of the moving object and the image burring of the static scene. Experiments with real infrared and simulated image sequences demonstrate that the proposed algorithm can achieve relative robust convergence speed and accurate correction result. In the proposed algorithm, the static area cannot be corrected well enough because of the smaller learning rate. Due to the lack of scene movement, some denoising methods may be used to process this area to improve the image quality in the future work. Moreover, reducing its computational complexity for hardware implementation is another necessary task.

Acknowledgements

We would like to express our sincere appreciation to the anonymous reviewers for their insightful and valuable comments, which have greatly helped us in improving the quality of the paper. This work is partially supported by the National Natural Science Foundation of China (61401343 and 61265006), the Fundamental Research Funds for the Central Universities of China (JDZD140202; WRYB142312; JDYB140105), and the 863 Program of China (2014AA8098089C).

Reference

[1] C. Zhang, W.Y. Zhao, Scene-based nonuniformity correction using local constant statistics, J. Opt. Soc. Am. A 25 (2008) 1444–1453.
[2] A. Friedenberg, I. Goldblatt, Nonuniformity two-point linear correction errors in infrared focal plane arrays, Opt. Eng. 37 (1998) 1251–1253.
[3] J.G. Harris, Y.M. Chiang, Nonuniformity correction of infrared image sequences using the constant-statistics constraint, IEEE T Image Process 8 (1999) 1148–1151.
[4] D.A. Scribner, K.A. Sarkady, J.T. Caulfield, M.R. Kruer, G. Katz, C.J. Gridley, C. Herman, Nonuniformity correction for staring IR focal plane arrays using scene-based techniques, Int. Soc. Opt. Photon. (1990) 224–233.

[5] C. Zuo, Q.A. Chen, G.H. Gu, W.X. Qian, New temporal high-pass filter nonuniformity correction based on bilateral filter, Opt. Rev. 18 (2011) 197–202.
[6] R.C. Hardie, M.M. Hayat, E. Armstrong, B. Yasuda, Scene-based nonuniformity correction with video sequences and registration, Appl. Opt. 39 (2000) 1241–1250.
[7] B.M. Ratliff, M.M. Hayat, R.C. Hardie, An algebraic algorithm for nonuniformity correction in focal-plane arrays, J. Opt. Soc. Am. A 19 (2002) 1737–1747.
[8] D.A. Scribner, K.A. Sarkady, M.R. Kruer, J.T. Caulfield, J.D. Hunt, C. Herman, Adaptive nonuniformity correction for IR focal-plane arrays using neural networks, Int. Soc. Opt. Photon. (1991) 100–109.
[9] S.N. Torres, M.M. Hayat, Kalman filtering for adaptive nonuniformity correction in infrared focal-plane arrays, J. Opt. Soc. Am. A 20 (2003) 470–480.
[10] A. Averbuch, G. Liron, B.Z. Bobrovsky, Scene based non-uniformity correction in thermal images using Kalman filter, Image Vis. Comput. 25 (2007) 833–851.
[11] Y.-J. Liu, H. Zhu, Y.-G. Zhao, Nonuniformity correction algorithm of infrared focal plane arrays based on particle filters, Infrared Laser Eng. 6 (2008) 004.
[12] K.M. He, J. Sun, X.O. Tang, Guided image filtering, IEEE T Pattern. Anal. 35 (2013) 1397–1409.
[13] E. Vera, S. Torres, Fast adaptive nonuniformity correction for infrared focal-plane array detectors, Eurasip. J. Appl. Sig. P. (2005). 1994–2004.
[14] A. Rossi, M. Diani, G. Corsini, Bilateral filter-based adaptive nonuniformity correction for infrared focal-plane array systems, Opt. Eng. 49 (2010).
[15] E. Vera, P. Meza, S. Torres, Total variation approach for adaptive nonuniformity correction in focal-plane arrays, Opt. Lett. 36 (2011) 172–174.